Internal Wave Interactions with Equatorial Deep Jets. Part II: Acceleration of the Jets

JOANNA E. MUENCH

Seattle, Washington

ERIC KUNZE

Applied Physics Laboratory, University of Washington, Seattle, Washington

(Manuscript received 19 January 1999, in final form 11 October 1999)

ABSTRACT

What drives the equatorial deep jets is a puzzle because of their isolation from surface forcing by the intervening main pycnocline and the Equatorial Undercurrent, and from lateral boundaries by distances of tens of thousands of kilometers. It would take decades for energy to propagate to the jets' midbasin location from boundary sources. Their persistence points to some mechanism maintaining them in situ. The authors hypothesize that the ambient internal wave field deposits momentum fluxes at critical layers within the deep jets and, using calculated momentum- and energy-flux divergences as forcing, estimate acceleration of the mean zonal flow in the deep jets. Internal wave momentum-flux divergences are more than sufficient to sustain the jets, acting to sharpen the shear between the jets on timescales of months to years. Predicted energy-flux divergences produce turbulent dissipation rates compatible with those observed.

1. Introduction

Some basic characteristics of the Pacific equatorial deep jets are well established (Firing 1987; Ponte and Luyten 1989; Muench et al. 1994). The jets form vertically alternating layers of ± 5 cm s^{-1} zonal flow with vertical wavelengths of 300–500 m straddling $\pm 2°$ of the equator. They span the depth range 500–3000 m, insulated from the surface by the Equatorial Undercurrent and the main pycnocline. In the Pacific, where they have been best measured, they are zonally coherent over at least 10° longitude (Ponte and Luyten 1989) and steady on timescales of at least two years (Eriksen 1985). Their zonal velocity reverses at $\pm 1.5°$ latitude and potential vorticity anomalies are associated with them, properties of first-meridional-mode equatorially trapped long Rossby waves with zonal group velocities $Cg_x = N/[(2n + 1)k_z]$ (O'Neill and Luyten 1984; Muench et al. 1994) rather than long Kelvin waves (Eriksen 1980; McCreary and Lukas 1986; Ponte and Luyten 1989).

However, what generates or maintains the deep jets is still unknown. Wind forcing (Wunsch 1977) cannot explain their deep penetration (McCreary 1984; McCreary and Lukas 1986), which would require multiple reflections off the eastern and western boundaries, taking decades to set up (Ponte and Luyten 1989). Even waves generated on the eastern boundary (Ponte 1989) would take a decade to reach the central equatorial Pacific where jets have been observed. Neither can these sources explain the jets' narrow vertical wavenumber band. The isolation from plausible external forces suggests that there must be some local mechanism sustaining the jets.

Various modes of instability have been investigated (L. M. Rothstein 1999, personal communication; Rowe 1996). Hua et al. (1997) showed that structure closely resembling the jets is a natural outcome of equatorial inertial instability, $f\Pi \leq 0$ (where Π is the potential vorticity) and that energy will cascade from smaller instability scales to deep-jet wavelengths. They also argued that the meridional shear $U_y > 0$ across the equator was unstable using data from Firing (1987). However, as shown by Muench et al. (1994), the deep jets dominate potential vorticity anomalies and U_y on the equator.

High dissipation rates found in the shear zones between the jets would erode the jets in $\Delta t = E/\varepsilon = 6$–$10$ yr, where E is the jet energy and ε the observed turbulent kinetic energy dissipation rate (Gregg et al. 1995). This is an underestimate of Δt if the jets are not the source of the turbulence as argued here.

Muench and Kunze (1999, referred to as Part I) pos-

Corresponding author address: Eric Kunze, APL, University of Washington, 1013 NE 40th, Seattle, WA 98105-6698.
E-mail: kunze@ocean.washington.edu

tulate that the elevated dissipation rates between the deep jets arose from internal wave critical layers. They quantify the magnitude and structure of the momentum- and energy-flux divergences due to an isotropic Garrett and Munk internal wave field set at 3° latitude (Munk 1981) and encountering critical layers within the jets (their Fig. 8, reproduced here in Fig. 2). Crude estimates suggest that the magnitude of the momentum-flux divergence is sufficient to significantly accelerate the deep jets.

In this paper, we examine the forced response more rigorously by applying the Muench and Kunze (1999) estimates for momentum-flux divergences that take into account shadowing by adjacent jets and spectral replenishment within and between the jets to an analytic model for the acceleration and cross-stream circulation of a jet. We also investigate the sensitivity of the model to plausible changes in the momentum-flux divergence.

a. Theoretical background

Central to understanding how waves interact with a mean flow is the ''noninteraction'' theorem. This theorem was proven more than 35 years ago for planetary Rossby waves in geostrophic shear (Eliassen and Palm 1961) and since then generalized to other wave–mean flow systems (Charney and Drazin 1961; Holton 1974; Andrews and McIntyre 1976; Boyd 1976; Dunkerton 1980). It states that, given a linear inviscid harmonic wave field, there is no net acceleration of the mean flow, and no net change of the mean background density structure, in the absence of forcing, damping, or critical layers. The wave field may drive an Eulerian circulation but, in the absence of irreversible processes, Eulerian and wave transports exactly balance (Boyd 1976) so that no net Lagrangian transport of properties occurs. This theorem imposes important restrictions on the impact of a wave field on a background flow.

Other studies of wave–mean flow interactions have considered damping by Rayleigh friction and Newtonian cooling so that wave fluxes are no longer conserved (Andrews and McIntyre 1976; Boyd 1976; McPhaden et al. 1986; Proehl 1990). In this paper, we will conserve wave fluxes except at critical layers; that is, we assume that conditions for the noninteraction theorem are violated only at critical layers. Critical-layer interactions produce (i) acceleration or deceleration of the mean flow through deposition of internal wave momentum flux, as well as (ii) possible frictional deceleration due to mixing of momentum arising from turbulence generated by energy-flux divergences.

b. Prior results

Previous oceanographic investigations of wave–mean flow interactions have focused on acceleration by a single forcing term in the momentum equations. Following an atmosphere model by Jones and Houghton (1971), Ruddick (1980) balanced the vertical momentum-flux divergence with acceleration of the mean flow,

$$\frac{\partial U}{\partial t} = -\frac{\partial \langle u'w' \rangle}{\partial z},$$

where the angle brackets denote a time mean, primes are second-order wave quantities, and the $\partial U/\partial t$ refers to wave-driven mean acceleration. Kunze and Müller (1989) argued that, by analogy to surface wind stress forcing, the momentum-flux divergence is directly balanced by the Coriolis term,

$$f\tilde{v} = \frac{\partial \langle u'w' \rangle}{\partial z}.$$

This result requires that there are no horizontal gradients to the momentum-flux divergence, so no Ekman pumping. A more complete scale analysis (e.g., Charney 1973) reveals that forcing of a mean flow of finite extent by momentum-flux divergences requires consideration of more complete equations of motion. The Ruddick (1980) balance holds in the limit of tall narrow jets (aspect ratios $H/L \gg f/N$), and the Kunze and Müller balance in the limit of very broad flow.

The complete equations of motion are necessary here. Our approach is shown to be identical to the transformed Eulerian mean equations and the Eliassen–Palm formalism (Andrews et al. 1987) in the appendix. The Eliassen–Palm flux was developed in conjunction with the noninteraction theorem. It is often used as a diagnostic for wave–mean flow interactions in quasigeostrophic problems because of its unique definition under that scaling which links the momentum fluxes of a quasigeostrophic forcing eddy field to the meridional flux of potential vorticity, $\nabla \cdot \mathbf{F} = \langle v'q' \rangle$. No such link exists for internal gravity wave forcing (which has zero potential vorticity fluxes). Therefore, to keep the number of variables to a minimum, it is preferable to use momentum- and buoyancy-fluxes rather than Eliassen–Palm fluxes for our problem.

Separate forced equations are produced for the acceleration of the mean zonal flow and the cross-stream circulation induced by momentum-flux divergences of the internal wave field (section 2). We will use flux-divergence forcing from Muench and Kunze (1999), summarized in section 3. The first-order solution is presented first (section 4a). Solutions including O(Ro) terms (section 4b), and the effects of turbulent viscosity and diffusion (section 4c), are shown to differ little from the first-order solution. The resulting alongstream acceleration and across-stream circulation, as well as their implications, are discussed in the conclusions (section 5).

2. Method

a. Equations of motion

We begin our analysis by deriving the appropriate equations of motion. Observations of the deep jets show

that they are zonally coherent over at least 10° of latitude, implying a zonal wavelength Λ_x in excess of 10 000 km (Ponte and Luyten 1989). Therefore, we assume the background flow associated with the equatorial deep jets is unidirectional with $\partial/\partial x = 0$ and slowly varying in time, that is, $U(y, z, t)$.

We define a cross-stream mean circulation $(\tilde{v}, \tilde{w})$ induced by second-order fluctuating wave quantities, for example, v' such that $\langle v' \rangle = 0$ where the angle brackets denote a long-time average. Then, the equations of motion for mean background zonal velocity U, meridional velocity $\tilde{v}$, vertical velocity $\tilde{w}$, buoyancy B, and reduced pressure P are

$$\frac{\partial U}{\partial t} - (\beta y - U_y)\tilde{v} + U_z\tilde{w} = -\frac{\partial \langle u'v' \rangle}{\partial y} - \frac{\partial \langle u'w' \rangle}{\partial z} + \frac{\partial [\nu_e(y, z)U_z]}{\partial z} \tag{1}$$

$$\frac{\partial \tilde{v}}{\partial t} + \tilde{v}\frac{\partial \tilde{v}}{\partial y} + \tilde{w}\frac{\partial \tilde{v}}{\partial z} + \underbrace{\beta y U} = -\frac{\partial P}{\partial y} - \frac{\partial \langle v'^2 \rangle}{\partial y} - \frac{\partial \langle v'w' \rangle}{\partial z} \tag{2}$$

$$0 = -\frac{\partial P}{\partial z} + B \tag{3}$$

$$\frac{\partial B}{\partial t} + B_y\tilde{v} + \overline{N}^2\tilde{w} = -\frac{\partial \langle v'b' \rangle}{\partial y} + \frac{\partial [\kappa_e(y, z)B_z]}{\partial z} \tag{4}$$

$$\frac{\partial \tilde{v}}{\partial y} + \frac{\partial \tilde{w}}{\partial z} = 0, \tag{5}$$

where $\nu_e(y, z)$ and $\kappa_e(y, z)$ represent turbulent eddy viscosities and diffusivities. We assume that the meridional v-momentum equation remains in equatorial geostrophic balance [braced terms in (2)] (Lukas and Firing 1984) and the vertical w-momentum equation in hydrostatic balance (3), allowing us to relate deep equatorial jet zonal velocity U and buoyancy B through the equatorial thermal wind

$$\beta y U_z = -By.$$

This requires that the deep equatorial jets' timescale

$$t \gg (\beta y)^{-1} \sim (\beta L)^{-1} \sim 10 \text{ days},$$

where the equatorial radius of deformation $L = \sqrt{N\Lambda_z/(2\pi\beta)} = 68$ km. The observed jets have timescales exceeding 15 months (Firing 1987; Fig. 3 of Muench et al. 1994), justifying this assumption.

While, like midlatitude internal waves, the forcing equatorial internal wave field has been observed both to be invariant (Blumenthal 1987) and varying by a factor of 3 (Hayes 1981) on seasonal timescales, it seems likely that, averaged over a year, the equatorial internal wave field can be taken as invariant. Muench and Kunze (1999) use the Garrett and Munk (Munk 1981) internal wave field set at 3° latitude to impinge upon the jets. This model is horizontally isotropic. Unlike the GM76 model (Garrett and Munk 1975; Cairns and Williams 1976), its spectral level varies as f^{-1}. Additional discussion of variability in the equatorial internal wave field and its effect on the momentum-flux divergences can be found in the conclusions of Muench and Kunze (1999).

The buoyancy is defined as $\overline{B}(z) + B(y, z, t) + b' = -g\delta\rho/\rho_o$, where $\partial\overline{B}/\partial z = \overline{B}_z = N^2$ represents the background stratification, the overbar denotes a spatial average over the region of interest, $B(y, z, t)$ perturbations are due to the deep equatorial jets including the wave-induced background buoyancy perturbation, and b' is the fluctuating wave buoyancy anomalies. The local buoyancy frequency N can be taken as constant in time and space in the vicinity of the deep jets (Muench et al. 1994), the jets inducing only weak perturbations to the background stratification.

We explicitly distinguish between momentum-flux deposition by internal waves at critical layers and mixing of momentum by turbulence generated by internal wave breaking at critical layers. The turbulent eddy viscosity $\nu_e(y, z)$ in (1) and eddy diffusivity $\kappa_e(y, z)$ in (4) arise from elevated turbulence generated at internal wave critical layers between the jets due to energy-flux divergences $\varepsilon = |\nabla \cdot (v'p')|$. The turbulent eddy viscosity can be estimated as

$$\nu_e(y, z) = -\frac{\langle u''w'' \rangle}{\sqrt{u_z'^2 + v_z'^2}} \simeq \frac{\varepsilon(y, z)}{u_z'^2 + v_z'^2} \leq \frac{\varepsilon(y, z)}{4N^2} \tag{6}$$

from the turbulent kinetic energy equation (Osborn 1980) since only wave shears $(u_z'^2 + v_z'^2) > 2N$ are large enough to give rise to turbulence (Miles and Howard 1961); shear associated with the equatorial jets U_z is far too weak to induce shear instability (Gregg et al. 1995), so cannot be directly responsible for the observed turbulence. The double-primed quantities are turbulent. The eddy diffusivity can be parameterized as

$$\kappa_e(y, z) = -\frac{\langle w''b'' \rangle}{N^2} = \frac{\gamma\varepsilon(y, z)}{N^2} \leq \frac{0.2\varepsilon(y, z)}{N^2} \tag{7}$$

where the "mixing efficiency" $\gamma \leq 0.2$ (Osborn 1980). Approximating the vertical shear by a critical Richardson number criterion Ri_c in (6) may overestimate the turbulent eddy viscosities since $\text{Ri} < \text{Ri}_c = 0.25$ for shear instability (Miles and Howard 1961). The turbulent kinetic energy dissipation rate $\varepsilon(y, z)$ is equated to the vertical energy-flux divergence at critical layers (Fig. 2a)

$$\varepsilon = \left| \frac{\partial \langle w'p' \rangle}{\partial z} \right|, \tag{8}$$

consistent with observations (Fig. 17 of Kunze et al. 1995). Parameterizations (6)–(8) capture the basic physics of turbulent mixing, if not the exact eddy viscosities and diffusivities.

b. Cross-stream streamfunction and alongstream acceleration

Some manipulation of (1)–(5) is necessary to determine how the momentum-flux divergences influence the zonal mean flow U. If the wave-induced accelerations of the mean zonal velocity U remain in thermal-wind balance (2), then we can define a geostrophic acceleration potential Φ such that

$$\frac{\partial U}{\partial t} = \frac{1}{\beta y}\frac{\partial \Phi}{\partial y}, \qquad \frac{\partial B}{\partial t} = -\frac{\partial \Phi}{\partial z} \tag{9}$$

and, from continuity (5), a cross-stream circulation streamfunction ψ can be defined such that

$$\tilde{v} = \frac{\partial \psi}{\partial z} \qquad \tilde{w} = -\frac{\partial \psi}{\partial y}. \tag{10}$$

While an acceleration potential is the simplest way to reduce the equations of motion into two governing equations in terms of Φ and ψ on a midlatitude f plane, the geometry of the equator adds an essential singularity to the partial differential equation for the acceleration potential Φ, making a solution using this approach problematic.

Instead, following McPhaden et al. (1986), a conservation equation for the cross-stream streamfunction ψ and a diagnostic equation for the alongstream acceleration $\partial U/\partial t$ can be formulated. Solving (1) and (4) for the cross-stream streamfunction ψ gives

$$\overline{N}^2\frac{\partial^2\psi}{\partial y^2} + \beta y(\beta y - U_y)\frac{\partial^2\psi}{\partial z^2} + 2\beta y U_z\frac{\partial^2\psi}{\partial y\partial z} + \beta U_z\frac{\partial\psi}{\partial z}$$
$$= \beta y\frac{\partial^2\langle u'v'\rangle}{\partial y\partial z} + \beta y\frac{\partial^2\langle u'w'\rangle}{\partial z^2} + \frac{\partial^2\langle v'b'\rangle}{\partial y^2}$$
$$- \beta y\frac{\partial^2[\nu_e U_z]}{\partial z^2} - \frac{\partial^2[\kappa_e B_z]}{\partial y\partial z}, \tag{11}$$

where flow curvatures, U_{yy}, U_{yz}, and U_{zz}, have been neglected. Should vertical and meridional shear terms prove significant, neglect of flow curvatures would have to be reevaluated. However, the O(Ro) terms prove to have little impact (section 4b), justifying their neglect. Assuming momentum-flux divergences are significant only in the vicinity of critical layers within the equatorial deep jets (Muench and Kunze 1999) implies that the cross-stream streamfunction is bounded in the far field ($\partial\psi/\partial y = \partial\psi/\partial z \to 0$ as $y \to \infty$). With the jets roughly symmetric about the equator and assuming symmetric forcing by the internal wave field, there is no reason to expect any cross-equatorial flow, so $\tilde{v} = \partial\psi/\partial z = 0$ at $y = 0$. Asymmetric forcing by internal waves, as might arise from asymmetry in atmospheric forcing (such as the tendency for the intertropical convergence zone to lie in the Northern Hemisphere), would invalidate this condition, but there is insufficient data at present to prescribe asymmetric forcing. Symmetric forcing is more appropriate, given our limited knowledge of the equatorial internal wave field.

Solving (11) for the cross-stream streamfunction ψ provides the wave-induced cross-stream circulation $(\tilde{v}, \tilde{w})$. Then, from (1), the zonal acceleration due to the momentum-flux divergences is given by

$$\underbrace{\frac{\partial U}{\partial t} = U_z\frac{\partial\psi}{\partial y} + (\beta y - U_y)\frac{\partial\psi}{\partial z} - \frac{\partial\langle u'v'\rangle}{\partial y} - \frac{\partial\langle u'w'\rangle}{\partial z} + \frac{\partial(\nu_e U_z)}{\partial z}}. \tag{12}$$

c. Application to the equatorial deep jets

The model background jets used in this study (Muench and Kunze 1999) are vertically sinusoidal and meridionally Gaussian:

$$U(y, z) = U_0 \exp\left[\frac{-y^2}{2L^2}\right]\cos\left(\frac{2\pi z}{\Lambda_z}\right)$$

(Fig. 1), where $L = 68$ km is the equatorial radius of deformation (Table 1). A Gaussian meridional structure incorrectly implies Kelvin wave dynamics, while Muench et al. (1994) demonstrated that the jets are better described as equatorially trapped long Rossby waves with off-equator flow reversals. However, momentum-flux divergences near the equator were found to be comparable when more realistic meridional structures were used in the simulations (Muench and Kunze 1999).

d. Scaling

Scaling arguments will help identify dominant terms in (11). We define a height scale $\Lambda_z/2\pi$, where $\Lambda_z = 330$ m is the vertical wavelength of Pacific jets (Table 1; Muench et al. 1994); vertical wavelengths of up to 500 m have been observed in the Indian (Luyten and Swallow 1976; Dengler and Quadfasel 2000, manuscript submitted to J. Phys. Oceanogr.) and Atlantic (Eriksen 1985; Ponte et al. 1990; Gouriou et al. 1999) oceans. A meridional lengthscale $L = \sqrt{N\Lambda_z/(2\pi\beta)} = 68$ km corresponds to the equatorial radius of deformation, and

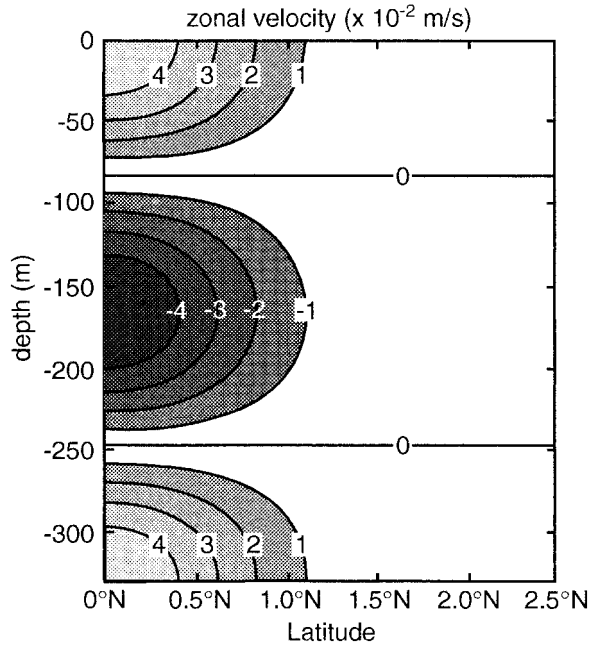

FIG. 1. The meridional and vertical structure of the zonal velocity for the model deep equatorial jets with vertical wavelength $\Lambda_z = 330$ m, meridional scale $L = 68$ km, and maximum zonal velocity $U = 5$ cm s^{-1}.

a zonal velocity scale $U = 0.05$ m s^{-1} (Table 1) is consistent with observations (Firing 1987). The background buoyancy frequency $N = 2 \times 10^{-3}$ rad s^{-1} can be taken as constant. Separating the effective Coriolis term into two parts, terms on the lefthand side of (11) scale as

$$1 : 1 : \frac{U}{\beta L^2} : \frac{U}{\beta L^2} : \frac{U}{\beta L^2}.$$

The last three terms are of order Rossby number $U/\beta L^2$, which is 0.5 in parts of the deep jets, so not small. Terms containing vertical shear U_z scale identically to those with meridional shear because the Froude number U_z/N and Rossby number $U_y/(\beta y)$ for the deep jets are identical,

$$\frac{U_z}{N} \sim \frac{2\pi U}{N\Lambda_z} = \frac{U}{\beta L^2} \sim \frac{U_y}{\beta y}.$$

This scaling is robust at the equator because $U_y \to 0$ at the same rate as $y \to 0$.

To scale the relative magnitudes of the momentum-flux terms on the righthand side of (11), we assume that momentum-flux divergences are proportional to gradients of the mean flow,

$$\frac{\partial \langle u'w' \rangle}{\partial z} \sim -C_{uw} U_z; \qquad \frac{\partial \langle u'v' \rangle}{\partial y} \sim -C_{uv} U_y;$$

$$\frac{\partial \langle v'b' \rangle}{\partial y} \sim -C_{vb} U_y,$$

TABLE 1. Parameter values for the equatorial deep jets.

U	0.05 m s^{-1}
N	2×10^{-3} rad s^{-1}
Λ_x	>10 000 km
Λ_z	330 km
L	68 km
$R_o = U/\beta L^2$	0.5
$Fr = U_z/N$	0.5

where the method of derivation of the constants of proportionality C_{ab} is described by Eqs. (10) and (11) of Muench and Kunze (1999). These parameterizations are developed for scaling purposes only and cannot be used to solve the complete problem because they do not accurately capture the degree of localization of the forcing terms (Fig. 2a). If scales appropriate for the deep jets are used (Table 1), then

$$\frac{2\pi L}{\Lambda} C_{uw} \gg C_{uv}, \frac{C_{vb}}{N}.$$

The $\langle v'b' \rangle$ correction to the residual streamfunction is $\langle v'b' \rangle / N^2 \sim O(C_{vb} U/N^2) = 8 \times 10^{-7}$ $L = 4 \times 10^{-2}$ m^2 s^{-1}, implying a correction to the residual meridional circulation $\tilde{v}$ of $O(0.1$ cm s$^{-1})$ as compared to $O(1$ cm s$^{-1})$ due to $\partial \langle u'w' \rangle / \partial z$. Therefore, the only forcing term that needs to be considered in this problem is divergence of the vertical flux of zonal momentum, $\partial \langle u'w' \rangle / \partial z$. This implies that the jets are broad.

3. Flux-divergence forcing

The momentum- and energy-flux divergences that arise from internal waves encountering critical layers in the equatorial deep jets were estimated by Muench and Kunze (1999) and are summarized here in Fig. 2. Muench and Kunze found jet geometry to be important for the structure and magnitude of the momentum-flux divergence. Jets of both longer and shorter vertical wavelengths were found to have weaker momentum-flux divergences (section 4d of Muench and Kunze)—longer wavelengths because there is more time for wave–wave interactions to spectrally replenish that part of the internal wave spectrum depleted by critical-layer interactions between and within the jets (thus restoring vertical symmetry and the tendency for up- and downgoing waves encountering critical layers to cancel each other)—shorter wavelengths because of greater shadowing. However, there are numerous assumptions and uncertainties in the flux divergences so they should be taken as order-of-magnitude estimates only.

Muench and Kunze's (1999) estimates of the vertical divergence of vertical momentum flux are reproduced in Fig. 2a. The divergence vanishes at jet centers and between the jets. Arms of positive momentum-flux divergence encircle westward jets while arms of negative flux divergence embrace eastward jets. Maximum flux-divergence magnitudes are found at $\pm 0.8°$ latitude

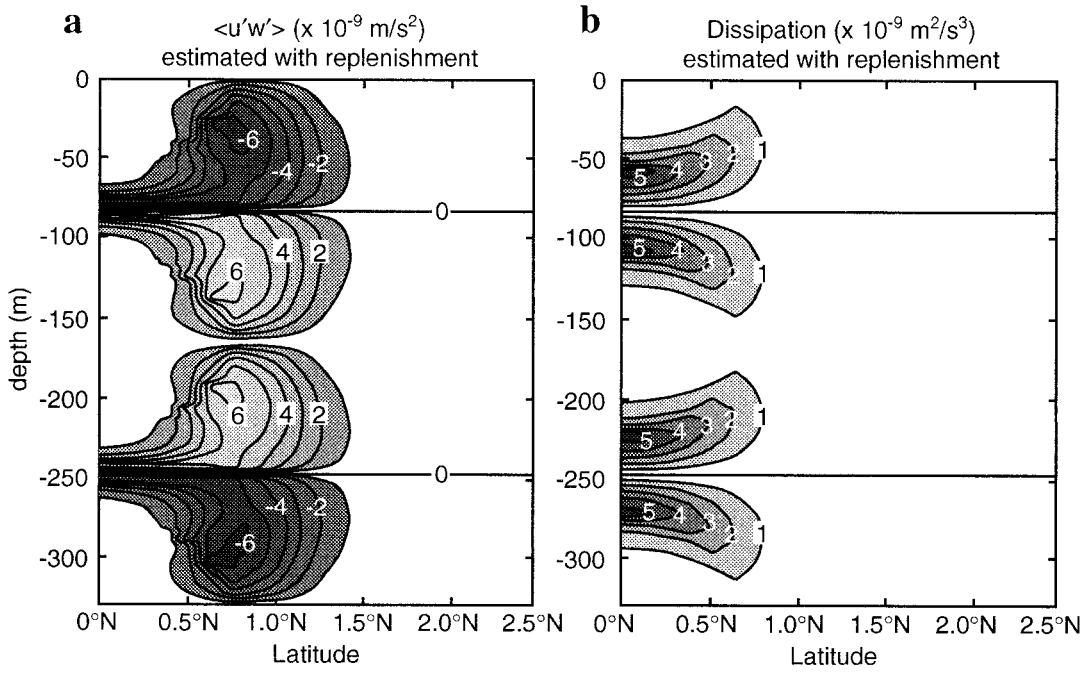

FIG. 2. Momentum-flux divergence $\partial\langle u'w'\rangle/\partial z$ (a) and energy-flux divergence $|\partial\langle w'p'\rangle/\partial z| = \varepsilon$ (b) estimates assuming the influence of shadow effects between the jets and allowing spectral replenishment of shadowed ray paths within each jet (from Muench and Kunze 1999).

above and below jet centers. The magnitude is sensitive to the spectral replenishment rate and the internal wave spectral level (section 4a), but the localized structure in Fig. 2a is a robust feature of the meridional and vertical structure of the jets.

The energy-flux divergence (Fig. 2b), equivalent to the turbulent dissipation rate ε (8), reaches a maximum of 5×10^{-9} W kg^{-1} localized in the high-shear layers between the jets. These values are consistent with observations (Gregg et al. 1995; K. Polzin 1999, personal communication). Energy-flux divergences are less pronounced on the lateral edges of the jets at $\pm 1°$ latitude.

4. Forcing with realistic estimates of $\langle u'w'\rangle$

For greater physical insight, we start with the first-order solutions of the cross-stream streamfunction ψ (11) and zonal acceleration $\partial U/\partial t$ (12). The O(Ro) terms will be included in section 4b. The first-order cross-stream streamfunction ψ is found by neglecting order-Rossby-number and turbulent viscous/diffusion terms in (11)

$$\frac{\partial^2\psi}{\partial y^2} + \frac{(\beta y)^2}{N^2}\frac{\partial^2\psi}{\partial z^2} = \frac{\beta y}{N^2}\frac{\partial^2\langle u'w'\rangle}{\partial z^2}, \tag{13}$$

which may be solved analytically if the momentum-flux divergence forcing is known and is of simple form (Muench 1995). Likewise, the u-momentum in Eq. (12) reduces to a simple balance between acceleration of the mean zonal flow $\partial U/\partial t$, meridional velocity $\tilde{v}$, and the vertical momentum-flux divergence

$$\frac{\partial U}{\partial t} - \beta y\tilde{v} = -\frac{\partial\langle u'w'\rangle}{\partial z}. \tag{14}$$

Equations (13) and (14) were solved using a simultaneous overrelaxation algorithm (Press et al. 1987).

a. *Momentum-flux divergences with spectral replenishment*

The cross-stream circulation is shown in Fig. 3b for the momentum-flux divergences from Muench and Kunze (1999), which include shadowing of rays by adjacent jets and spectral replenishment through internal wave–wave interactions between and within the jets (Fig. 2a). Maximum momentum-flux divergences are 1.6 cm s^{-1}/month (Fig. 2b). Comparison of Figs. 2a, 3a, and 3b shows that cross-stream flow tends to balance the flux-divergence off the equator, while zonal acceleration dominates on the equator. The circulation is localized and strongest on the edges of the jets, with maximum meridional velocities of $\tilde{v} = 0.5$ cm s^{-1} carrying fluid into the upper and lower edges of westward jets and out of the upper and lower edges of eastward jets. These Eulerian flows largely compensate the transport associated with the vertical divergence of vertical momentum-flux $\partial\langle u'w'\rangle/\partial z$ (Fig. 2a) off the equator. Approaching the equator, the Coriolis frequency $\beta y \to 0$ while

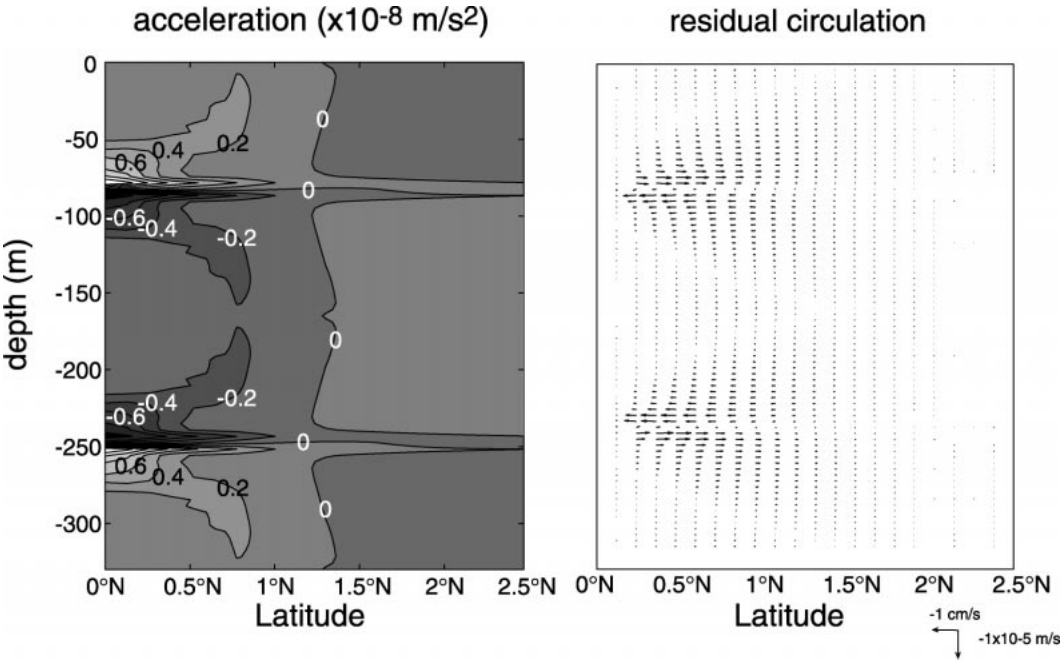

FIG. 3. Zonal acceleration $\partial U/\partial t$ (a) and residual cross-stream circulation $(\tilde{v}, \tilde{w})$ forced by the momentum-flux divergences shown in Fig. 2. Order-Rossby-number terms in (11) have been ignored. Contour intervals for zonal acceleration are 0.2×10^{-8} m s^{-2}. The tops and bottoms of the jets are accelerated in the sense of the jet flow so as to make the vertical structure more square-wave-like (Fig. 4). The cross-stream circulation carries water equatorward on the upper and lower edges of westward jets, poleward on the upper and lower edges of eastward jets. Vertical motion $\tilde{w}$ is into (out of) eastward (westward) jets on the equator but very weak because vertical scales for the momentum-flux divergence (Fig. 2a) are much smaller than the jet wavelengths Λ_z.

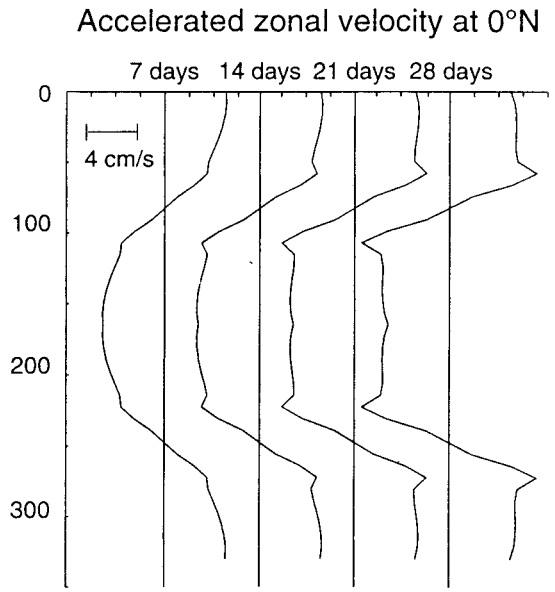

FIG. 4. Time evolution of vertical profiles of deep-jet zonal velocity $U(z)$ accelerated by internal wave momentum-flux divergences. The vertical structure of the jets goes from being sinusoidal to square-wave-like with intensified shear between the jets. If the accelerations shown in Fig. 3a are used, the time series spans one month with 7 days between profiles. If jet accelerations are reduced due to lower internal wave spectra and losses to other zonal shears on the equator (section 4d), the time series spans 1–2 years with 3–6 months between profiles.

$\tilde{v}$ remains finite, so the Coriolis term in (14) becomes negligible, leaving only the zonal acceleration $\partial U/\partial t$ to balance $\partial\langle u'w'\rangle/\partial z$.

The double-lobed acceleration structure (Fig. 3a) acts on the zonal velocity structure straddling the equator by accelerating the upper and lower edges of the jets at maximum rates of 1.6 cm s^{-1}/month. The upper and lower edges of westward jets accelerate westward, upper and lower edges of eastward jets eastward (Fig. 3a). The net effect is to sharpen the shear between the jets and make the vertical structure more square-wave-like (Fig. 4). Jet centers do not intensify or migrate. The maximum acceleration of 1.6 cm s^{-1}/month is large and comparable to $\beta y\tilde{v} = 1.5$ cm s^{-1}/month for $\tilde{v} = 0.5$ cm s^{-1} off the equator (Fig. 3b). By comparison, McPhaden et al. (1986) found accelerations of less 0.1 cm s^{-1}/month due to wind-forced Kelvin waves encountering critical layers in the equatorial undercurrent. Kelvin waves are not physically analogous to the problem described here because they are equatorially trapped and so blocked from interacting with interior jets by jets above and below. Internal waves overcome this by propagating meridionally as well as zonally.

Under the influence of internal-wave-induced acceleration, the jets become square-wave-like (Figs. 4 and 5). Sharpening is most pronounced on the equator (cf. Figs. 1 and 5). Based on the momentum-flux divergence

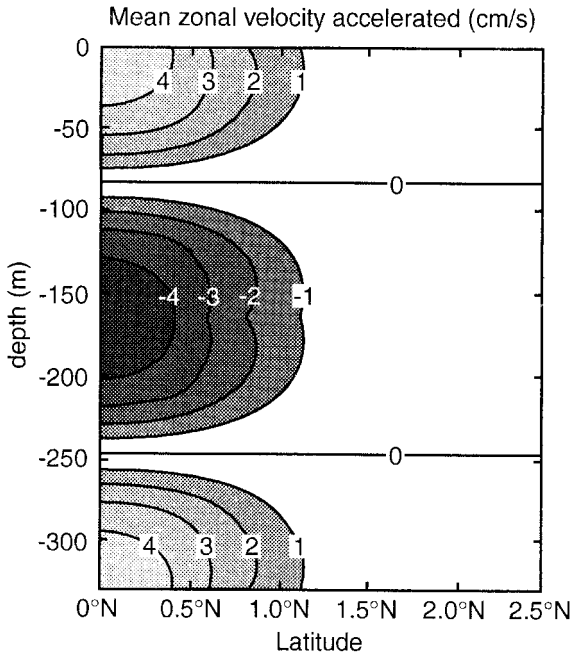

FIG. 5. Meridional/vertical structure of the deep-jet zonal velocity $U(y, z)$ after being accelerated for 2 days (one month) by the rate shown in Fig. 3a (1/15th the Fig. 3a rate, section 4d). The maximum zonal velocity does not change but the upper and lower edges of the jets accelerate on the equator, intensifying vertical shear between the jets.

in Fig. 2 (Muench and Kunze 1999), the jet vertical shear should become unstable, $U_z/N > 2$, in less than a month. This seems unrealistic given the observed steady nature of the jets.

Several factors could diminish the magnitude of forcing by momentum-flux divergences:

- reducing the internal wave spectral levels. We have used the Munk (1981) model for the GM spectrum with its f^{-1} dependence for variance as compared to the GM76 (Cairns and Williams 1976; Gregg and Kunze 1991) model with variance independent of f. Measurements of the finescale vertical wavenumber spectrum across the equator at 140°W and 156°E (Gregg et al. 1995) find spectral levels elevated above GM76 levels by factors of 2–3 at 3°N (where we set our impinging wave field), but smaller than the Munk (1981) level by factors of 3–5, so would reduce the momentum-flux divergences by the same amount.
- higher spectral replenishment rates would restore the depleted part of the internal wave field more rapidly, making it more symmetric and so diminishing the net momentum-flux divergences through compensation between up- and downgoing waves, particularly between the jets. Our replenishment rates are based on midlatitude studies (Müller et al. 1986), which may not be valid on the equator.
- erosion by turbulent friction and diffusion.
- other equatorial zonal shears depleting internal wave momentum fluxes at critical layers, leaving only a fraction available to interact with the jets.

These factors would impact the *magnitude* of the momentum-flux divergences but not their general structure. In the following sections, we explore some of the assumptions (Rossby number, turbulent mixing, spectral replenishment rates, other background shears) that went into our estimate of the momentum-flux divergence forcing and how these assumptions influence the magnitude of the acceleration. Only the first and last factors listed above will remain viable candidates for reducing the momentum-flux divergence to reasonable levels.

b. Including O(Ro) terms

Although the Rossby number for the jets is not small (Ro $\sim$ 0.5), inclusion of O(Ro) terms—that is, solving (11) and (12) rather than (13) and (14)—does not significantly alter the residual meridional velocity. Including O(Ro) terms [(11) rather than (13)] reduces the maximum meridional velocity by only 7% and does not shift the region of strongest cross-stream circulation. Using (12) rather than (14) to estimate the acceleration likewise produces no major changes; the acceleration increases by less than 1% because O(Ro) terms are only significant in 30-m-thick layers (one-tenth of a jet wavelength) between the jets in a limited $\pm 0.5°$ latitudinal band about the equator. Therefore, advection of the background shear by the cross-stream circulation is not important and the O(Ro) terms do not significantly alter the spatial structure of the zonal acceleration. Likewise, neglected nonlinear advection terms in the v-momentum equation (2) are only comparable to the retained geostrophic terms in small localized regions of the domain, so do not affect the overall balance significantly.

c. Including turbulent friction and diffusion

Viscous effects due to internal waves breaking and producing turbulence at critical layers will also influence the mean flow [(1)–(5)]. Using our estimate of a maximum dissipation rate of $\varepsilon = 10^{-8}$ W kg^{-1} (Fig. 2b), the maximum viscosity/diffusivity is $\nu_e \sim \kappa_e \sim \varepsilon/4N^2 \sim 6 \times 10^{-4}$ m^2 s^{-1} from (6) and (7), respectively. If, for the sake of argument, deceleration of the mean flow by turbulent friction is taken to be a first-order balance, we estimate a viscous decay rate $\Lambda_z^2/(4\pi^2\nu_e) = N^2\Lambda_z^2/(\pi^2\varepsilon^2) \sim$ 2–3 months for the jets, comparable to the rate at which internal wave momentum-flux divergences sharpen the jets. This is a gross underestimate because high dissipation rates are localized to small regions between the jets as shown in the next paragraph. Gregg et al. (1995) estimated a decay timescale on energetic grounds of $E/\varepsilon \sim$ 6–10 yr. This is also an underestimate since the jets are not the source of the turbulence.

The effect of the internal-wave-driven turbulent mix-

ing on the jets can be treated more rigorously by including the spatially variable diffusion coefficients in (14) as

$$\frac{\partial U}{\partial t} = \beta y \tilde{v} - \frac{\partial \langle u'w' \rangle}{\partial z} + \underbrace{\frac{\partial (\nu_e U_z)}{\partial z}} \tag{15}$$

and in (13) as

$$\frac{\partial^2 \psi}{\partial y^2} + \frac{(\beta y)^2}{N^2} \frac{\partial^2 \psi}{\partial z^2} = \frac{\beta y}{N^2} \frac{\partial^2 \langle u'w' \rangle}{\partial z^2} - \underbrace{\frac{\beta y}{N^2} \frac{\partial^2 (\nu_e U_z)}{\partial z^2} - \frac{1}{N^2} \frac{\partial^2 (\kappa_e B_z)}{\partial y \partial z}}, \tag{16}$$

where $\nu_e(y, z)$ and $\kappa_e(y, z)$ are given by (6) and (7), respectively, using Fig. 2b energy-flux divergences. Turbulent viscosities and diffusivities will also influence the structure of the internal wave momentum-flux divergence, but this is a still higher-order effect that is neglected here. Inclusion of turbulent viscous and diffusion terms, that is, solving (15) and (16), does not visibly alter the zonal acceleration. While the dissipation rate is large between the jets, the velocity and energy there is small. Dissipation rates are small in the jet centers. Thus, inclusion of turbulent friction drains little energy from the jets. Decay times are $O(100$ yr).

Elevated turbulent dissipation rates observed in other equatorial shears (Gregg et al. 1995) will increase the overall background dissipation rate. Scale analysis suggests that decelerations produced by these increased dissipation rates are $\sim O(3 \times 10^{-3}$ cm s^{-1}/month), corresponding to decay times of 300 years. Therefore, the effects of turbulent friction and mixing are insignificant compared to the momentum-flux divergence.

d. Interactions with other shears

Muench and Kunze (1999) discuss interactions between the internal gravity wave field and background equatorial shears other than the deep jets in their conclusions. High dissipation rates are found in all regions of high local shear, not just shear associated with the deep jets (Gregg et al. 1995). Unlike the steady deep jets, the random isotropic nature of these other shears will produce no net mean momentum-flux divergence. Nevertheless, these localized events will deplete the internal wave momentum-flux available to interact with the jets.

According to Ponte and Luyten (1989), the deep jets account for about 20% of the total variance in the zonal velocity vertical wavenumber spectrum over the depth range of the jets. The other dominant spectral peak was at a vertical wavelength of 560 m. This peak was associated with motions of 3–6 yr period and 10 000-km zonal wavelength that they attributed to meridionally symmetric long Rossby waves. If shears other than the deep jets provide a sink for 80% of the internal wave energy, then momentum-flux divergences in the deep jets will be reduced by a factor of 5 from those shown in Fig. 2a. Taken together with the factor of 3–5 overestimation of internal wave forcing using the Munk (1981) internal wave model (section 4a), acceleration of the jets could be reduced by over an order of magnitude, approaching more reasonable values of 1 cm s^{-1}/yr (Figs. 4 and 5).

5. Conclusions

We have explored deposition of internal wave momentum at critical layers in the jets as a possible mechanism for maintaining the equatorial deep jets. In Part I, Muench and Kunze (1999) quantify the momentum- and energy-flux divergences expected from a Garrett and Munk internal wave field (Munk 1981) propagating equatorward from $\pm 3°$ latitude and encountering critical layers within the jets (Fig. 2a). Account was made for shadowing by neighboring jets and spectral replenishment of the internal wave spectrum through wave–wave interactions (Müller et al. 1986) between and within the jets.

Equating energy-flux divergences to turbulence production rates implies maximum turbulence dissipation rates of 5×10^{-9} W kg^{-1} (Fig. 2b), consistent with microstructure measurements. Turbulent friction and mixing have negligible impact on the deep jets because they are confined to thin layers in the shear zones between the jets. As energy-flux divergences would arise even in the presence of perfectly compensating up- and downgoing momentum fluxes, they only provide an upper bound constraint on the momentum-flux divergences.

Momentum-flux divergences due to internal wave critical layers within the equatorial deep jets are more than sufficient to maintain the jets. These accelerations act to make the vertical structure on the equator more square-wave-like (Fig. 4). Jet centers do not intensify or migrate, but shear between the jets sharpens (Figs. 4 and 5). These intensifying shears might ultimately break down into turbulence through shear instability ($U_z/N > 2$), weakening the background shear, or cascade upscale to jet wavelengths as argued by Hua et al. (1997). The O(Ro) terms in (11) and (12) were found to have negligible impact on acceleration of the jets. This implies that terms involving background flow curvature can be neglected as well so that the simpler diagnostic equations for cross-stream streamfunction (13) and geostrophic acceleration (14) can be used.

The magnitude of the inferred accelerations indicates that this forcing mechanism cannot be ignored despite its uncertainties. In fact, the 1.6 cm s^{-1}/month accelerations of the upper and lower edges of the jets based on the momentum-flux divergences in Fig. 2a are clearly excessive given the steady nature of the jets in two years of observations (Firing 1987). Several processes could

reduce the momentum-flux divergences and geostrophic acceleration to more plausible levels:

(i) observed internal wave levels at 3°N (Gregg et al. 1995) are a factor of 3–5 weaker than predicted by the Munk (1981) internal wave spectral model used by Muench and Kunze (1999). This would reduce the momentum-flux divergences by a comparable amount.
(ii) critical-layer interactions with the other background shears that account for 80% of the zonal flows at the equator (Ponte and Luyten 1989) would deplete the internal wave field and reduce momentum-flux divergences in the deep jets by a factor of 5.
(iii) higher spectral replenishment rates would diminish the difference between up- and downgoing waves encountering critical layers, thus reducing the net momentum-flux divergences; if spectral replenishment was complete and instantaneous, there would be no net momentum-flux divergence and no acceleration of the mean flow. It has been suggested that spectral replenishment rates at the equator are lower than the midlatitude rates we have used (M. C. Gregg 1999, personal communication) but this has not yet been tested rigorously.

Taken together, (i) and (ii) would reduce internal wave momentum-flux divergences (Fig. 2a) and geostrophic accelerations (Fig. 3a) by more than an order of magnitude to more reasonable values of 0.5–1 cm s^{-1}/yr. Thus, shear between the jets is sharpening at a sufficient rate to produce shear instability $U_z > 2N$ in 1–2 years. Both longer and shorter jet wavelengths were found to have diminished momentum-flux divergences (section 4d of Muench and Kunze), possibly insufficient to maintain scales other than those observed against turbulent erosion. Longer wavelengths allow more spectral replenishment between critical layers which symmetrizes the up- and downgoing internal wave fields. Shorter wavelengths have reduced momentum-flux divergences because of greater shadowing. Alternatively, Hua et al. (1997) argued that equatorial instabilities on scales shorter than those of the jets cascade energy upscale to jet wavelengths.

With this picture of how the equatorial deep jets might persist, questions remain about the origin of these giant coherent structures. Given their long Rossby wave character (Muench et al. 1994), implying westward energy propagation, clues might be found on the eastern boundary along the continental slope of South America. However, the strong positive feedback associated with internal wave momentum-flux divergences maintaining existing jets may obscure such origins. Alternatively, Hua et al.'s (1997) work suggests that structure like that of the equatorial deep jets is a natural outcome of instability on the equator, so could arise in situ from forcing by a variety of sources including but not limited to the deposition of momentum-flux at the internal wave critical layers described here.

Acknowledgments. We thank Mike Gregg for sharing his insights into the nature of equatorial internal wave and turbulence fields. Kurt Polzin and John Toole generously made available their recent observations from the equatorial Atlantic. E. K. thanks Peter Müller for valuable input on the wave–mean flow interaction problem. Charlie Eriksen, David Battisti, and an anonymous reviewer provided helpful comments on the manuscript. This research was carried out with support from NASA Grant NGT-30035 and NSF Grant OCE-90-19580.

APPENDIX

Equivalence to the Eliassen–Palm Flux Approach

Atmospheric scientists and some equatorial oceanographers have approached the question of wave–mean flow interaction using Eliassen–Palm fluxes in the transformed Eulerian-mean equations (Andrews and McIntyre 1976; McPhaden et al. 1986; Proehl 1990). While appropriate for the atmosphere, some of the approximations made to the transformed Eulerian-mean equations by these authors are not appropriate for our application. However, with approximations appropriate for the deep jets, the two approaches will be shown to be equivalent in this appendix.

We first define a residual wave-induced mean meridional circulation

$$\tilde{v}^* = \tilde{v} - \frac{1}{N^2}\frac{\partial\langle v'b'\rangle}{\partial z} \tag{A1}$$

$$\tilde{w}^* = \tilde{w} + \frac{1}{N^2}\frac{\partial\langle v'b'\rangle}{\partial y}. \tag{A2}$$

This transformation removes meridional and vertical velocities associated with compensating Eulerian mean and wave-induced transports. These effects are small for the deep jets but are included here to illustrate the development of this method. Substituting (A1) and (A2) into (1)–(5), the transformed Eulerian-mean (TEM) equations are

$$\frac{\partial U}{\partial t} - (\beta y - U_y)\tilde{v}^* + U_z\tilde{w}^* = \nabla\cdot\mathbf{F} \tag{A3}$$

$$\beta y U = -\frac{\partial P}{\partial y} \tag{A4}$$

$$0 = -\frac{\partial P}{\partial z} + B \tag{A5}$$

$$\frac{\partial B}{\partial t} + B_y\tilde{v}^* + \overline{N}^2\tilde{w}^* = -\frac{B_y}{N^2}\frac{\partial\langle v'b'\rangle}{\partial z} \tag{A6}$$

$$\frac{\partial\tilde{v}^*}{\partial y} + \frac{\partial\tilde{w}^*}{\partial z} = 0, \tag{A7}$$

where the Eliassen–Palm flux vector $(0, F_y, F_z)$ is given by

$$F_y = \frac{U_z}{\overline{N}^2}\langle v'b'\rangle - \langle u'v'\rangle \tag{A8}$$

$$F_z = \frac{(\beta y - U_y)}{\overline{N}^2}\langle v'b'\rangle - \langle u'w'\rangle. \tag{A9}$$

The jet zonal velocity U, including the wave-induced mean perturbation, is assumed to remain in thermal-wind balance with the buoyancy to leading order (A4); that is, accelerations are assumed to be weak.

We define a residual cross-stream streamfunction χ such that

$$\tilde{v}^* = \frac{\partial \chi}{\partial z}, \qquad \tilde{w}^* = -\frac{\partial \chi}{\partial y}, \tag{A10}$$

which represents the cross-stream circulation *not compensated* for by wave-induced momentum fluxes, that is, the net cross-stream transport. The equations of motion then become

$$\frac{\partial U}{\partial t} - (\beta y - U_y)\frac{\partial \chi}{\partial z} - U_z\frac{\partial \chi}{\partial y} = \nabla \cdot \mathbf{F} \tag{A11}$$

$$\frac{\partial B}{\partial t} - \beta y U_z\frac{\partial \chi}{\partial z} - N^2\frac{\partial \chi}{\partial y} = -\frac{B_y}{N^2}\frac{\partial \langle v'b'\rangle}{\partial z}. \tag{A12}$$

Using the assumed geostrophic nature of the residual zonal flow, a governing equation for the cross-stream streamfunction may be found:

$$N^2\frac{\partial^2 \chi}{\partial y^2} + \beta y(\beta y - U_y)\frac{\partial^2 \chi}{\partial z^2} + 2\beta y U_z\frac{\partial^2 \chi}{\partial y \partial z} + \beta U_z\frac{\partial \chi}{\partial z} = -\beta y\frac{\partial(\nabla \cdot \mathbf{F})}{\partial z} - \frac{\beta y U_z}{N^2}\frac{\partial^2 \langle v'b'\rangle}{\partial y \partial z} - \frac{\beta U_z}{N^2}\frac{\partial \langle v'b'\rangle}{\partial z}, \tag{A13}$$

where $B_y = -\beta y U_z$. With the transformation, $\chi = \psi - \langle v'b'\rangle/N^2$, and neglecting turbulent friction and diffusion, this equation is identical to (11). The induced acceleration of the zonal flow may now be found by solving for χ in (A13) and using (A11) to obtain $\partial U/\partial t$. The scaling for the left-hand side of (A13) is identical to that of (8) and implies that $\chi \simeq \psi$.

Were the induced cross-stream circulation small, allowing neglect of the residual meridional and vertical velocities in (A3), a simple balance between the acceleration of the zonal flow and the Eliassen–Palm flux divergence would be possible. Under these conditions, the Eliassen–Palm flux approach is useful because it allows for direct estimate of the acceleration from the momentum-flux divergences. Andrews and McIntyre (1976) showed that this was appropriate in the limit of high background Richardson number (Ri $\gg$ 1). However, this is not an appropriate scaling for our problem where momentum-flux diverences act both to accelerate the mean zonal flow and form a cross-stream circulation.

The Eliassen–Palm approach removes compensating Lagrangian transports from the residual mean cross-stream circulation when those effects are large and reveals when cancellation between flux-divergence terms occurs due to the nonacceleration theorem. However, for our problem, in which Lagrangian transports are small, using the Eliassen–Palm flux divergence to represent the forcing obscures the fact that only the vertical momentum-flux divergence contributes significantly to the acceleration of the zonal jets, so neither simplifies the physics nor provides insight into the problem.

REFERENCES

Andrews, D. G., and M. E. McIntyre, 1976: Planetary waves in horizontal and vertical shear: The generalized Eliassen–Palm relation and the mean zonal acceleration. *J. Atmos. Sci.,* **33,** 2031–2048.

——, J. R. Holton, and C. B. Leovy, 1987: *Middle Atmosphere Dynamics.* Academic Press, 489 pp.

Blumenthal, M. B., 1987: Interpretation of equatorial current meter data as internal waves. Ph.D. thesis, WHOI, Woods Hole, MA, 371 pp.

Boyd, J. P., 1976: The noninteraction of waves with the zonally averaged flow on a spherical earth and the interrelationships of eddy fluxes of energy, heat, and momentum. *J. Atmos. Sci.,* **33,** 2285–2291.

Cairns, J. L., and G. O. Williams, 1976: Internal wave observations from a midwater float, 2. *J. Geophys. Res.,* **81,** 1943–1950.

Charney, J. G., 1973: Planetary fluid dynamics. *Dynamic Meteorology,* P. Morel, Ed., Reidel, 97–352.

——, and P. G. Drazin, 1961: Propagation of planetary-scale disturbances from the lower into the upper atmosphere. *J. Geophys. Res.,* **66,** 83–109.

Dunkerton, T., 1980: A Lagrangian mean theory of wave/mean-flow interaction with applications to nonacceleration and its breakdown. *Rev. Geophys. Space Phys.,* **18,** 409–418.

Eliassen, A., and E. Palm, 1961: On the transfer of energy in stationary mountain waves. *Geofys. Publ.,* **22**(3), 409–418.

Eriksen, C. C., 1980: Evidence for a continuous spectrum of quatorial waves in the Indian Ocean. *J. Geophys. Res.,* **85,** 3285–3303.

——, 1985: Moored observations of deep low-frequency motions in the central Pacific Ocean: Vertical structure and interpretation as equatorial waves. *J. Phys. Oceanogr.,* **15,** 1085–1113.

Firing, E., 1987: Deep zonal currents in the cental equatorial Pacific. *J. Mar. Res.,* **45,** 791–812.

Garrett, C. J. R., and W. H. Munk, 1975: Space–time scales of internal waves: A progress report. *J. Geophys. Res.,* **80,** 291–297.

Gouriou, Y., B. Bourlès, H. Mercier, and R. Chuchla, 1999: Deep jets in the equatorial Atlantic Ocean. *J. Geophys. Res.,* **104,** 21 217–21 226.

Gregg, M. C., and E. Kunze, 1991: Shear and strain in Santa Monica basin. *J. Geophys. Res.,* **96,** 16 709–16 719.

——, D. P Winkel, T. B. Sanford, and H. Peters, 1995: Turbulence produced by internal waves in the oceanic thermocline at mid- and low latitudes. *Dyn. Atmos. Oceans,* **24,** 1–14.

Hayes, S. P., 1981: Vertical fine structure observations in the eastern equatorial Pacific. *J. Geophys. Res.,* **86,** 10 983–10 999.

Holton, J. R., 1974: Forcing of mean flows by stationary waves. *J. Atmos. Sci.,* **31,** 942–945.

Hua, B. L., D. W. Moore, and S. le Gentil, 1997: Inertial nonlinear equilibration of equatorial flows. *J. Fluid Mech.,* **331,** 345–371.

Jones, W. L., and D. D. Houghton, 1971: The coupling of momentum between internal gravity waves and mean flow: A numerical study. *J. Atmos. Sci.,* **28,** 604–608.

Kunze, E., and P. Müller, 1989: The effect of internal waves on vertical geostrophic shear. *Parameterization of Small-Scale Pro-*

cesses: Proceedings 'Aha Huliko'a Hawaiian Winter Workshop, Hawaii Inst. Geophys. Spec. Publ., 271–285.

——, R. W. Schmitt, and J. M. Toole, 1995: The energy balance in a warm-core ring's near-inertial critical layer. *J. Phys. Oceanogr.*, **25,** 942–957.

Lukas, R., and E. Firing, 1984: The geostrophic balance of the Pacific Equatorial Undercurrent. *Deep-Sea Res.,* **31,** 61–66.

Luyten, J. R., and J. C. Swallow, 1976: Equatorial undercurrents. *Deep-Sea Res.,* **23,** 999–1001.

McCreary, J. P., 1984: Equatorial beams. *J. Mar. Res.,* **42,** 395–450.

——, and R. Lukas, 1986: The response of the equatorial ocean to a moving wind field. *J. Geophys. Res.,* **91,** 11 691–11 705.

McPhaden, M. J., J. A. Proehl, and L. M. Rothstein, 1986: The interaction of equatorial Kelvin waves with realistically sheared zonal currents. *J. Phys. Oceanogr.,* **16,** 1499–1515.

Miles, J. W., and L. N. Howard, 1961: On the stability of heterogeneous shear flows. *J. Fluid Mech.,* **10,** 496–512.

Muench, J. E., 1995: Internal wave interactions with equatorial deep jets. Ph.D. dissertation, University of Washington, Seattle, WA, 152 pp.

——, and E. Kunze, 1999: Internal wave interactions with equatorial deep jets: Part I. Momentum-flux divergences. *J. Phys. Oceanogr.,* **29,** 1453–1467.

——, ——, and E. Firing, 1994: The potential vorticity structure of equatorial deep jets. *J. Phys. Oceanogr.,* **24,** 418–428.

Müller, P., G. Holloway, F. Henyey, and N. Pomphrey, 1986: Nonlinear interactions among internal gravity waves. *Rev. Geophys.,* **24,** 493–536.

Munk, W. H., 1981: Internal waves and small-scale processs. *Evolution of Physical Oceanography,* B. A. Warren and C. Wunsch, Eds., The MIT Press, 264–291.

O'Neill, K., and J. R. Luyten, 1984: Equatorial velocity profiles. Part II: Zonal component. *J. Phys. Oceanogr.,* **14,** 1842–1852.

Osborn, T. R., 1980: Estimates of the local rate of vertical diffusion from dissipation measurements. *J. Phys. Oceanogr.,* **10,** 83–89.

Ponte, R. M., 1989: A simple model for deep equatorial zonal currents forced at lateral boundaries. *J. Phys. Oceanogr.,* **19,** 1881–1891.

——, and J. Luyten, 1989: Analysis and interpretation of deep equatorial currents in the central Pacific. *J. Phys. Oceanogr.,* **19,** 1025–1038.

——, ——, and P. L. Richardson, 1990: Equatorial deep jets in the Atlantic Ocean. *Deep-Sea Res.,* **37,** 711–713.

Press, W. H., B. P. Flannery, S. A. Teukolsky, and W. T. Vetterling, 1987: *Numerical Recipes: The Art of Scientific Computing.* Cambridge University Press, 818 pp.

Proehl, J. A., 1990: Equatorial wave–mean flow interaction: The long Rossby waves. *J. Phys. Oceanogr.,* **20,** 274–294.

Rowe, D., 1996: Eddy forcing of sub-thermocline equatorial mean flow. Ph.D. dissertation, University of Rhode Island, Narragansett, RI, 101 pp.

Ruddick, B. R., 1980: Critical layers and the Garrett–Munk spectrum. *J. Mar. Res.,* **38,** 135–145.

Wunsch, C., 1977: Response of an equatorial ocean to a periodic monsoon. *J. Phys. Oceanogr.,* **7,** 497–511.